Wide-range absolute photodetachment spectrum of NO_2^-

S. B. Woo, E. M. Helmy,* P. H. Mauk, and A. P. Paszek
Department of Physics, University of Delaware, Newark, Delaware 19711
(Received 27 October 1980; revised manuscript received 20 March 1981)

Dye-laser photodetachment of the electronic and vibrational ground state of NO_2^- is accomplished in a mass-identified drifted tube. Photodetached electrons are detected. The absolute-magnitude photodetachment spectrum is determined in the visible range of 5400 to 4350 Å and the ultraviolet range between 3550 and 2600 Å. The size of the cross section varies by more than 3 orders of magnitude when the size of the lowest vibrational transition is compared with that of the total cross section at ultraviolet energies. The electron affinity of NO_2^- is determined to be $E_A(NO_2^-) = 2.275 \pm 0.025$ eV. A Franck-Condon factor analysis of the absolute-magnitude spectrum yields, for the first time, structural constants of NO_2^- in the free gas phase. They are $r = 1.15 \pm 0.02$ Å and $\theta = 119.5° \pm 1.0°$. The solar detachment rate of NO_2^- is 0.042 ± 0.010 sec^{-1}. A peroxy isomer of NO_2^- is not detected.

I. INTRODUCTION

This paper reports a dye-laser photodetachment study of NO_2^- of C_{2v} symmetry

$$X\,^1A_1\,NO_2^- + h\nu \rightarrow X\,^2A_1\,NO_2 + e^- .$$

Our experiment has the following characteristics.

(1) It detects photodetached electrons. This gives unambiguous identification of the photodetachment process as opposed to photodestruction or photodissociation processes.

(2) The ions are created in a mass-identified drift tube operating under conditions of high pressure, long drift distance, and low E-to-N ratio (electric field strength to neutral gas-number density). This provides ion-mass identification and thermalization of ion temperatures to room temperature. A Boltzmann-distribution calculation shows that about 98% of the molecular ions are in the ground electronic and vibrational states, thereby facilitating theoretical interpretation of data.

(3) A multipass laser configuration is used to set up a large ion-photon interaction volume (about 6 cm^3). This keeps the effective number of photons per laser pulse high while maintaining low laser intensity to avoid multiphoton and/or nonlinear effects. The above arrangement coupled with a large collector area (about 12 cm^2) yields a respectable signal-to-noise ratio even when the size of the cross section is less than 10^{-20} cm^2. It makes possible photodetachment measurements in the ultraviolet range where the laser intensity drops off by a factor of about 20 owing to frequency doubling. The availability of data over a wide photon-energy range is another factor which is helpful in the theoretical interpretation of the data.

(4) The relative photodetachment measurements can be put on an absolute scale by comparison to O^-.

The four characteristics described above combine to establish a wide-range absolute photodetachment spectrum (WRAPS) which serves a complementary role to the existing threshold photodetachment spectrometry[1] and negative-ion photoelectron spectrometry.[1]

The existing work includes the absolute cross-section measurement of Warneck[2] and Vanderhoff[3] using beam techniques, the wide photon range relative cross-section measurement of Richardson *et al.*[4] using an ion-cyclotron-resonance technique, and the first dye-laser photodetachment of NO_2^- by Herbst *et al.*[5] In a pioneering work, Herbst *et al.* did a remarkable theoretical simulation of NO_2^- photodetachment at 2500 K, based on an absolute apparent cross section measured from an NO_2^- beam at an ion temperature of about 1500 to 2000 K and structural constants of NO_2^- determined from studies of nitrite ions in interactive environments. Smith *et al.*[6] did a coarse grid laser *photodestruction* measurement of NO_2^- using a swarm technique. The measurements were correctly identified as photodetachment, since the photon energies used were below the photodissociation threshold of about 4 eV.[7] They established an approximate threshold energy of 2.5 eV.

II. THE EXPERIMENT

Figure 1 gives a schematic diagram of this experiment. It shows a mass-identified drift tube with Brewster windows. The pressure to the left of the metal diaphragm D is a few torr and that to the right of D is less than 10^{-4} torr.

One or more species of negative ions are produced in a pulsed cold-cathode discharge ion source. They are guided by a weak electric field through a thermalizing region A toward the first shutter S_1 which is biased to stop the ions from traveling further down the drift tube. The pulse sequence shown in Fig. 1 describes the ion selection process. Pulse P_1 opens shutter S_1 admitting

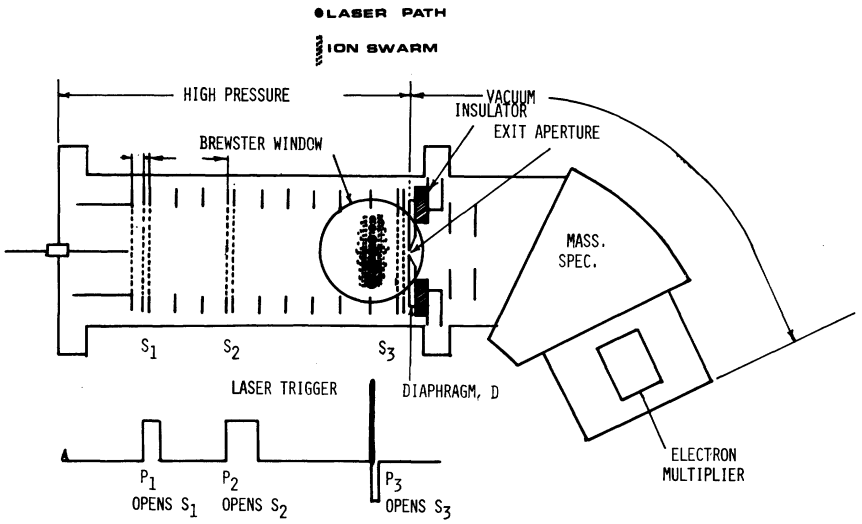

FIG. 1. Schematic diagram showing the dye-laser experiment in a mass-identified drift tube. The laser trigger pulse is timed such that the multiple laser beams traverse the ion swarm at its peak intensity.

ions into the ion selection region B. A desired ion species is selected by time of drift to pass through a second shutter S_2 opened by pulse P_2, to enter the primary drift region which is 6 cm in length. When the ions reach the ion-photon interaction region, located centrally between the Brewster windows, the laser is fired. The photodetached electrons are let through the third shutter S_3 by the application of pulse P_3. The electrons are collected by a metal diaphragm D which is about 4 cm in diameter and is electrically connected to a PAR™ Model 135 electrometer. The diaphragm is gold O-ring sealed to a supermica insulator plate which in turn is gold O-ring sealed to a metal plate welded to a Varian flange. The duration of P_3 is normally less than 15 μs so that photodetached electrons, being about two orders of magnitude faster than the anions, will have ample time to reach and pass through S_3, while the anions will not. The duration of the laser pulse is 1 μs.

If mass identification is desired, the diaphragm is disconnected from the electrometer and connected to a power supply floating on the ion-acceleration voltage of the mass spectrometer. The area of the pinhole at its center, 12 mils in diameter, serves as the collector area for the mass spectrometer. The mass spectrometer uses a channeltron electron multiplier. The mass number of the anion in our experiment is 46.

A CMX-4 pulsed dye laser provides photons in the 7300 to 4350 Å range, and after frequency doubling in the 3650 to 2650 Å range. The bandwidth is 3 cm^{-1} in the visible. The beam diameter is about 3 mm at the output mirror. Its divergence (half-angle) is about 1 milliradian so that the beam diameter has doubled by its 6th pass through the drift tube (see Fig. 1).

The multipass configuration is set up with two 99.7% reflectivity mirrors placed outside of the Brewster windows of the drift tube. Seven sets of mirrors are required to cover the 7300–2650 Å spectral range. Six passes are arranged as shown in Fig. 1. The 6th pass, after traversing the drift tube, is intercepted by a polished stainless-steel reflector and directed to a spectrometer to determine the wavelength to ±2 Å. The laser trigger time is so selected that the photons encountered the peak intensity of the ion swarm which has approximately a Gaussian shape in the drift direction and a zeroth-order Bessel function shape in the radial direction. This is for the purpose of extracting a maximum signal.

Ninety-nine-percent-purity NO gas manufactured by Matheson (500 psi tank) is admitted to the drift tube through a cold trap maintained at −90 °C. The pressure in the drift tube is monitored by an MKS Baratron capacitance manometer. The analog output from the electrometer is digitized and logged into a TRS-80 minicomputer. A laser on-and-off and a multicycled short-period-integration technique[8] are used to improve the signal-to-noise ratio and to eliminate background.

Laser power is determined by a Scientech power meter Model 36001. Whenever necessary, the laser intensity is kept low so that less than 3% of the NO_2^- is photodestructed. Less than 10% of O^- is photodestructed in the calibration experiment. This practice makes nonlinear and multiphoton effects insignificant in the determination of the absolute photodetachment cross section of NO_2^-.

III. DATA

The relative photodetachment measurements are made at 1.22 torr, $E/p = 10$ volt/cm torr, and 20 °C. Before entering the ion-photon interaction volume, the ions are thermalized through about 10^5 collisions. The thermalization time is about 0.5 ms. The relative photodetachment cross section σ^R as a function of wavelength λ is determined by

$$\sigma^R_{NO_2^-}(\lambda) = \frac{N_e(\lambda)}{n_p(\lambda)}, \tag{1}$$

where N_e and n_p are, respectively, the number of detected photodetached electrons and the number of photons. The relative measurements are placed on an absolute scale by calibration with respect to O^- photodetachment measurements of Branscomb *et al.*[9,10] O^- is created in O_2 in the same drift tube under identical pressure and E/N conditions. The absolute photodetachment cross section $\sigma(\lambda)$ is determined by

$$\sigma_{NO_2^-}(\lambda) = \sigma^R_{NO_2^-}(\lambda)\left(\frac{\sigma_{O^-}(\lambda')}{\sigma^R_{O^-}(\lambda')}\right)\left(\frac{\rho^P_{O^-}}{\rho^P_{NO_2^-}}\right), \tag{2}$$

where λ' and ρ^P are, respectively, the wavelength at which the calibration is done and ion-number density at the peak of the ion swarm which are different for the two ion species.

In pulsed drift experiments, the arrival time spectrum $I(t)$ is

$$I(t) = C\int_t^{t+(T_3-T_f)} \rho(t)\,v\,dt$$

$$\cong \rho(t)\,v(T_3 - T_f) \quad \text{for } (T_3 - T_f) \text{ small}, \tag{3}$$

where C, v, T_3, and T_f are, respectively, a multiplicative constant, the drift velocity, the opening time of shutter S_3, and the drift time through S_3. Hence the maximum ion-density ratio of peak ion densities in Eq. (3) can be determined in terms of measurable quantities:

$$\frac{\rho^P_{O^-}}{\rho^P_{NO_2^-}} = \frac{I^P_{O^-} v_{NO_2^-}(T_3 - T_f)_{NO_2^-}}{I^P_{NO_2^-} v_{O^-}(T_3 - T_f)_{O^-}}. \tag{4}$$

Figures 2 and 3 show, respectively, the absolute magnitude photodetachment spectrum of NO_2^- in the visible and uv range established using Eqs. (2) and (4). The mobilities required in the application of Eq. (4) are 3.5 volt cm torr^{-1} for O^- in O_2 and 1.8 for NO_2^- in NO. The error bars in our data represent the quadratic sum of one standard deviation statistical error and a combined estimated systematic error. The combined systematic fractional error is about 5% in the visible range and 10% in the ultraviolet range. In addition, there exists a zero-base uncertainty of $+2\times10^{-21}$ cm^2 and -0.5×10^{-21} cm^2.

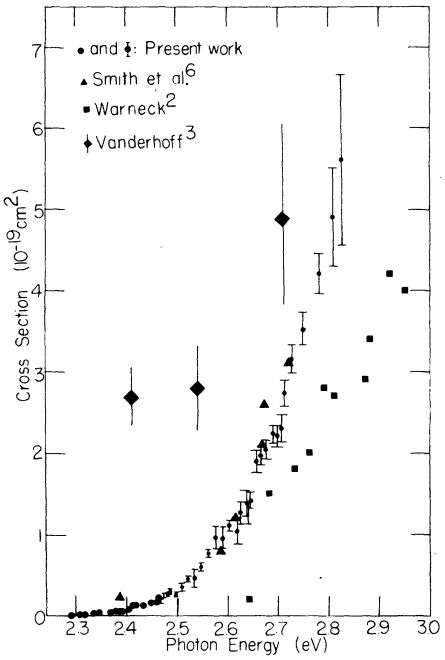

FIG. 2. Photodetachment cross section of NO_2^- in the visible region is shown.

A major contributor to the systematic error is the lack of precision in the positioning of the laser paths with respect to the peak of the ion swarms. Other contributions to the systematic errors include inaccuracies in the measured drift velocities, T_3, T_f, and l^P which enter into Eq. (4).

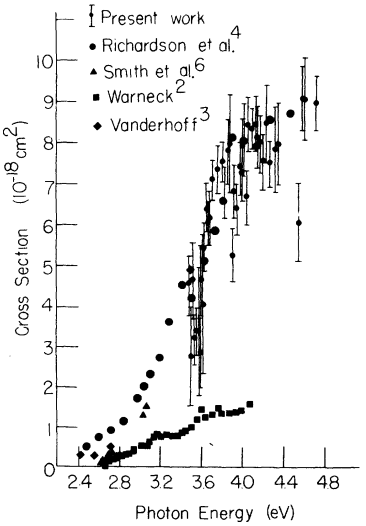

FIG. 3. Photodetachment cross section of NO_2^- measured in the uv range is shown. Data by others are also shown. Data by Richardson *et al.* have a resolution of about 0.4 eV in the uv range and 0.2 eV in the visible.

Depletion of NO_2^- due to the photodissociation, $NO_2^- + h\nu \rightarrow NO + O^-$, which begins at about 4.1 eV is ignored, because laser output above 4.1 eV is so weak that the depletion would be less than 1% if one assumes a huge dissociation cross section of 10^{-17} cm^2. Similarly, an erroneous photodetachment signal resulting from the photodetachment of those O^- ions, which are created in the above dissociation process, can be ignored.

Figure 2 shows the cross-section spectrum in the visible energy range which has steplike structures. They are associated with the onset of various vibrational transitions (see Sec. IV). It also shows that WRAPS permits the measurement of an absolute cross section as small as 5×10^{-21} cm^2. Data by other workers are shown. The energy resolution of Warneck's data is about 0.3 eV. Measurements by Smith *et al.*[6] and Vanderhoff[3] were done with lasers.

Figure 3 shows the cross section in the uv region. Steplike structures are no longer evident, since at 3.5 eV the sum of the Franck-Condon factors of the accessible vibrational channels is already about unity. New vibrational cross sections which emerge above this energy will be small in absolute magnitude when compared with the statistical fluctuation of the measured total cross section in the uv energy range. However, the shape and magnitude of the cross section in the uv range is valuable. It gives an indication of the cross section's energy dependence at energies for which the threshold laws[11-13] are no longer expected to apply. The large photon-energy range available in WRAPS permits experimental determination of this functional dependence. Data by Smith *et al.*,[6] Vanderhoff,[3] Warneck,[2] and the wide-range, low-resolution (0.2 to 0.4 eV) relative photodetachment measurement of Richardson *et al.*[4] are also shown. For comparison purposes, we arbitrarily normalize Richardson's data to our data at 4.4 eV. The two dips in the cross section seen in the data of Richardson *et al.* happen to coincide quite well with the present article. We assume that the total cross section in the uv range is a smooth function of the energy and that the similarities arise out of a statistical accident. Our visible data are not shown in this diagram to avoid cluttering.

In summary, our data shown in Figs. 2 and 3 provide some physical insight. The shape of the cross section in the uv range provides information on energy dependence of the cross section beyond the threshold, while the visible spectrum provides cross-section behavior at the threshold. The absolute magnitudes of both spectra, particularly the steplike structure in the visible region, determine the absolute magnitude of each of the Franck-Condon factors.

IV. THEORETICAL ANALYSIS

The total photodetachment cross section as a function of the photon energy is shown in Eq. (5),

$$\sigma(E) = \sum_{i=0}^{n} s_i(E) F_i , \tag{5}$$

where s_i is the partial cross section corresponding to a vibrational transition from the $X\,^1A_1$ electronic and (0, 0, 0) vibrational state of NO_2^- to the $X\,^2A_1$ electronic and ith higher vibrational excited state of NO_2. F_i is the Franck-Condon factor corresponding to such a transition. Transitions to the next higher electronic state $^2B_1$ of NO_2 will not occur, since it is about 3 eV above its ground state of $X\,^2A_1$.[14]

The Franck-Condon factors can be determined by a least-squares fit to the experimental data. They can also be calculated, using a harmonic approximation, for a given set of structural constants of NO_2^- consisting of the bond angle θ, the bond length r. The calculation of Franck-Condon factors requires the following data and assumptions: (1) Both $X\,^1A_1$ NO_2^- and $X\,^2A_1$ NO_2 are nonlinear molecules of symmetry C_{2v}, which have three normal modes of vibration, called symmetric stretching (ν_1), bending (ν_2), and asymmetric stretching (ν_3); (2) the harmonic approximation is valid; (3) the precise structural and spectral constants of NO_2 are known; (4) the spectral and force constants of NO_2^- are roughly known.

Then

$$F_i(\nu_1', \nu_2', \nu_3' \leftarrow 0, 0, 0) = \delta_{\nu_3' 0} \left(\int\int \psi^*_{\nu_1'}(Q_1') \psi^*_{\nu_2'}(Q_2') \psi_{\nu_1}(Q_1) \psi_{\nu_2}(Q_2)\, dQ_1\, dQ_2 \right)^2 , \tag{6}$$

where primed variables represent NO_2 and unprimed variables represent NO_2^-. The normal coordinates Q' and Q are related through the matrix expression:

$$Q' = (L'^{-1} Z L)\, Q + L'^{-1} R . \tag{7}$$

The definition for the various symbols used in Eqs. (6) and (7) are those used in Refs. 5 and 16, and will not be reproduced here.

The partial cross sections s_i are assumed to possess an $(E - E_i)^{1/2}$ threshold behavior[11-13] since a $p\pi$ electron departs from NO_2^- during photode-

tachment.[5] E_i is the threshold energy required for transition from (0, 0, 0) of NO_2^- to ith higher vibrationally excited state of the neutral. The dipole moment of NO_2 is only about 0.32 debye.[15] It does not seem sufficiently large to affect the $(E-E_i)^{1/2}$ threshold behavior.[16] This assumption is later supported by the results of least-squares fits which yield larger reduced χ^2 for $(E-E_i)^{1/3}$ or $(E-E_i)^{1/4}$ threshold behavior. Hence,

$$s_i(E)=\sigma_0 E(E-E_i)^{1/2} \times[1+A(E-E_i)+B(E-E_i)^2]H(E-E_i), \quad (8)$$

where σ_0 is a multiplicative factor. $H(E-E_i)$ is the Heaviside step function. A and B are coefficients of higher power terms which affect the nonthreshold behavior of the cross section.

For the least-squares-fit adjustment of the electron affinity E_A it is more convenient to express E_i as

$$E_i=E_A+\Delta E_i, \quad (9)$$

where ΔE_i is the energy difference between the ith higher vibrational state and $(0',0',0')$ of the neutral. Values of ΔE_i are well established (see Table I).

Substitution of Eqs. (8) and (9) into Eq. (5)

$$\sigma(E)=\sigma_0\sum_{i=0}^{n} E(E-E_A-\Delta E_i)^{1/2}[1+A(E-E_A-\Delta E_i)+B(E-E_A-\Delta E_i)^2]F_i H(E-E_A-\Delta E_i). \quad (10)$$

In principle, a non-linear-least-squares-fit program can be written to fit Eq. (10) to the visible and uv photodetachment spectrum by the adjustment of σ_0, E_A, A, B, and the Franck-Condon factors. In practice, however, such a nonlinear fit involving more than ten parameters should prove to be extremely difficult to handle, if at all manageable. We used physical insight to simplify the task to two steps of linear-least-squares fits.

A. Linear-least-squares fit in the visible and uv to determine σ_0, A and B

The wide range in photon energy available in the combined visible and ultraviolet spectra enables the determination of the shape of the partial cross sections beyond the threshold. That is, sufficient information is present for the determination of parameters A and B in Eq. (8). Since the cross sections are measured in absolute values, one may deduce not only the shape but also the absolute magnitude of s_i. That is, σ_0 can also be determined.

The computer program, which determines σ_0, A, and B, is described briefly below. For any given set of structure constants of NO_2^-, (r,θ), the theoretical Franck-Condon factors f_i can be calculated. Using calculated values of f_i, known values of ΔE_i (see Table I), a standard linear-least-squares fit to Eq. (10) is done to evaluate σ_0, A, B, $\Delta\sigma_0$, ΔA, and ΔB for an assumed value of E_A. A corresponding reduced χ^2, called $\chi^2_{r,\theta,\text{vis+uv}}$, is calculated. Maps of $\chi^2_{r,\theta,\text{vis+uv}}$ as a function of (r,θ) and E_A are made. Values of (σ_0, A, B) together with respective uncertainties are stored as a function of (r,θ) and E_A for use in the next series of linear-least-squares fit described below.

TABLE I. Spectral and structure constants of NO_2 ($^2A_1$) and NO_2^- ($^1A_1$).

	NO_2 (gas phase)	NO_2^- (interactive environment)	NO_2^- (gas phase)
ν_1 (cm^{-1})	1320[a]	1332[c]	
ν_2 (cm^{-1})	750[a]	821[c]	
ν_3 (cm^{-1})	1617.75[a]	1240[c]	
f_{11} (mdyn/Å)	12.43[a]	9.85[c]	
f_θ/r^2 (mdyn/Å)	1.0968[a]	1.7[c]	
$f_{\theta d}/r^2$ (mdyn/Å)	0.535	0.505[c]	
r ($N-O$) (Å)	1.1934[b]	1.236 ± 0.014[d]	1.15 ± 0.02[e]
θ ($\sphericalangle O-N-O$)	134.1°[b]	$115.4\pm1.73°$[d]	$119.5\pm1.0°$[e]

[a] E. T. Arakawa and A. H. Nielsen, J. Mol. Spectrosc. 2, 413 (1958).
[b] G. R. Bird, J. C. Baird, A. W. Jache, J. A. Hodgeson, R. F. Curl, Jr., A. C. Kunkle, J. W. Bransford, J. Rastrup-Andersen, and J. Rosenthal, J. Chem. Phys. 16, 442 (1948).
[c] R. E. Weston, Jr. and T. F. Brodasky, J. Chem. Phys. 27, 683 (1957).
[d] G. B. Carpenter, Acta Crystallogr. 8 852–833 (1955).
[e] Present work.

B. Linear-least-squares fit to the visible spectrum to determine (r,θ) and E_A

The steplike structure in the visible spectrum permits a least-squares fit to determine the experimental Franck-Condon factors F_i corresponding to various vibrational transitions. Values for σ_0, A, and B required in Eq. (10) are now available in the computer as a function of (r,θ) and E_A. For each set of (σ_0, A, B) and a corresponding E_A, a linear-least-squares fit to Eq. (10) is done. This time only the cross-section data in the visible spectrum are used. What comes out of the least-squares fit is a set of experimentally determined Franck-Condon factors F_i and their corresponding uncertainties ΔF_i. Each set of these F_i corresponds to a particular set of (E_A, r, θ).

The goodness of each least-squares fit to the visible spectrum is reflected in its reduced χ^2, designated as $\chi^2_{r,\text{vis}}$. The closeness of agreement between the experimentally determined F_i and the theoretical f_i of the same set of (r,θ) is evaluated according to the following criterion:

$$\chi^2_{\text{FC}} = \sum_i \frac{(F_i - f_i)^2}{\Delta F_i} .$$

Maps of $\chi^2_{r,\text{vis}}$ vs (E_A, r, θ) and maps of χ^2_{FC} vs (E_A, r, θ) are established.

V. ELECTRON AFFINITY, STRUCTURE CONSTANTS, AND PARTIAL CROSS SECTION OF NO_2^-

Figure 4 shows χ^2_{FC} as a function of r and θ at $E_A = 2.275$ eV. It shows two relative minima. The lower minimum occurs at $r = 1.15$ Å and $\theta = 119.5°$. It is well defined. A 1% change in either r or θ from the center of the minimum causes a factor of 2 increase in the χ^2_{FC}. Figure 5 shows χ^2_{FC}, $\chi^2_{r,\text{uv+vis}}$, and $\chi^2_{r,\text{vis}}$ as a function of E_A. Columns 1–4 of Table II show the close agreement of the experimental Franck-Condon factors F_i and the calculated ones at $r = 1.15$ Å and $\theta = 119.5°$,

We interpret the above to mean that the bond length and bond angle of NO_2^- in the gas phase are, respectively, 1.15 ± 0.02 Å and $119.5° \pm 1.0°$. In setting these uncertainties, we took into account (1) the statistical uncertainties reflected in Fig. 4, (2) the estimated systematic error due to a zero base uncertainty discussed in Sec. III, and (3) the neglect of vibrationally excited NO_2^- (about 2%) in the data analysis. Figure 4 shows that at the limits of the combined uncertainties of the structure constants the χ^2_{FC} is a factor of 5 or more larger than that at the minimum. The negative-ion structure constants determined in these experiments are quite accurate, despite the modest statistical

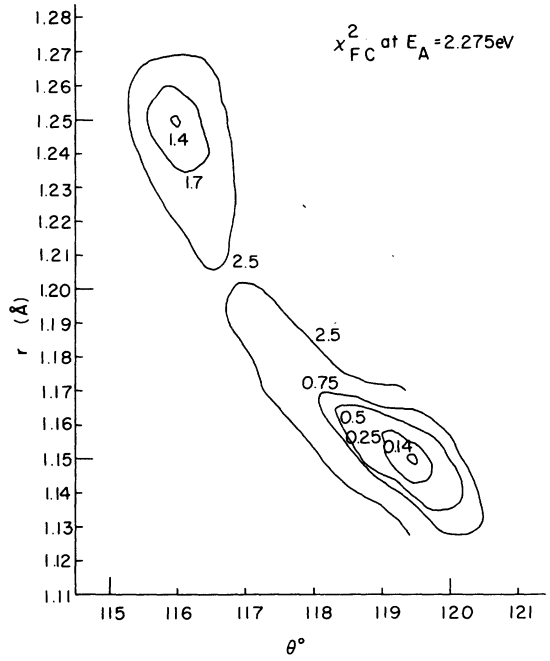

FIG. 4. Locus of χ^2_{FC} in the (r,θ) plane at $E_A = 2.275$ eV.

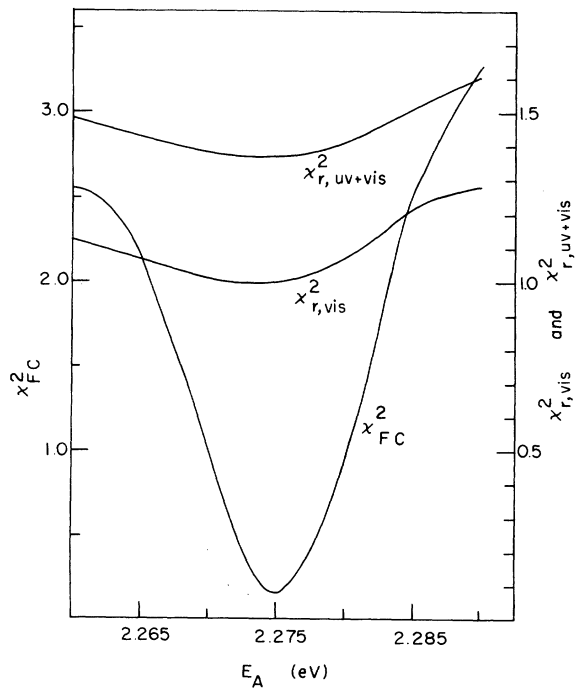

FIG. 5. χ^2_{FC}, $\chi^2_{r,\text{vis}}$, and $\chi^2_{r,\text{uv+vis}}$ as a function of E_A at $r = 1.15$ Å and $\theta = 119.5°$.

TABLE II. Calculated and fitted Franck-Condon factors for transitions in the visible spectrum seen in Fig. 2.

Transitions in order of increasing energy (0,0,0) ↓ (0,ν_2',0)	(0,0,0) ↓ $\nu_1' \neq 0$ (ν_1',ν_2',0)	r=1.15 Å, θ=119.5° Calculated $f_i \times 10^3$	Fitted $F_i \times 10^3$	$\frac{\Delta F}{F_i}$	r=1.25 Å, θ=116° Calculated $f_i \times 10^3$
(0,0,0)		3.01	2.92	0.32	3.04
(0,1,0)		15.5	15.8	0.15	15.7
	(1,0,0)	2.02	2.06	0.15	3.96
(0,2,0)		38.9	39.2	0.12	39.4
	(1,1,0)	11.3	11.4	0.12	19.2
(0,3,0)		63.2	61.1	0.15	63.8
	(2,0,0)	0.73	0.70	0.15	2.68
	(1,2,0)	30.6	29.6	0.15	45.1
(0,4,0)		74.6	76.9	0.25	75.1
	(2,1,0)	4.35	4.48	0.25	12.2
	(1,3,0)	53.7	55.3	0.25	68.2
(0,5,0)		68.2	55.5	1.02	68.5
	(3,0,0)	0.18	0.15	1.02	1.25
	(2,2,0)	12.7	10.3	1.02	26.9
	(1,4,0)	68.5	55.7	1.02	74.6

$$\chi^2_{FC} = \sum \left(\frac{F_i - f_i}{\Delta F_i} \right)^2 = 0.137$$

accuracy of the data shown in Figs. 2 and 3. The uncertainty in the data leads to rather large uncertainties in the Franck-Condon factors reported in Table II, but these uncertainties do not produce equally large uncertainties in the structure constants. Very small changes in r and/or θ produce very large alterations in the Franck-Condon factors. For example, a 1.8% increase in r at r = 1.15 Å and θ = 119.5° will cause a 60% or larger decrease in all the Franck-Condon factors in the (0, 0, 0→ 0, ν_2', 0) progression seen in Table II. Thus, these structural quantities are much more accurately determined than at first might be suggested by the appearance of the data.

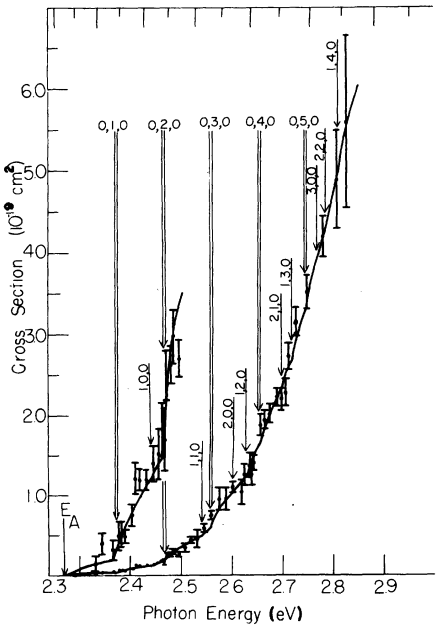

FIG. 6. Comparison of measured photodetachment cross section in the visible region with the theoretical curve based on fitted parameters of the partial cross section and Franck-Condon factors.

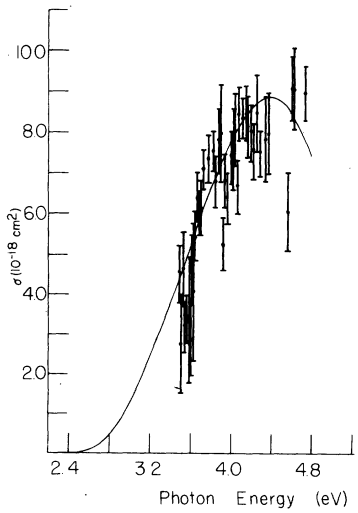

FIG. 7. Comparison of measured photodetachment cross section in the uv range with the theoretical curve.

The electron affinity is 2.275 ± 0.025 eV. The uncertainty is the quadratic sum of the statistical uncertainty seen in Fig. 5 and a systematic uncertainty of 0.020 eV which accounts for the differences in the rotational energy of the negative ion and neutral at $T = 300$ K.

One might note that χ^2_{FC} at the minimum is as small as 0.137. This justifies the linear-least-squares-fit procedure described in Sec. IV A which uses theoretical Franck-Condon factors as input values in the determination of σ_0, A, and B. One might also note that the magnitude of $\chi^2_{r,\,vis}$ and $\chi^2_{r,\,vis+uv}$ are about unity as expected.

Figure 6 shows that the experimental data in the visible spectrum and the results of the least-squares fit are in good agreement. The data and the fitted curve below 2.5 eV are also shown increased by a factor of 10. Threshold energies, at which various vibrational transitions occur, are indicated by arrows. Thresholds where $(0, 0, 0) \rightarrow (0, \nu_2', 0)$ transitions occur are indicated by the long arrows. Those where $(0, 0, 0) \rightarrow (\nu_1', \nu_2', 0)$ transitions occur, when $\nu_1' \neq 0$, are indicated by short arrows. Transitions for which $\Delta\nu_3 \neq 0$ can be ignored on theoretical grounds[5,16] and are therefore not included in the analysis. Figure 7 shows that the data and the results of the least-squares fit are in good agreement in the uv energy range as well. Our fitted curve is in good agreement with the experimental measurements of Richardson *et al.*[4] seen in Fig. 3, if one takes into account that their energy resolution is about 0.3 eV.

Values for σ_0, A, and B corresponding to our recommended values of r, θ, and E_A, are respectively, $(7.08 \pm 0.21) \times 10^{-19}$ cm^2 eV$^{3/2}$, (3.27 ± 0.15) eV^{-1}, and (-1.50 ± 0.09) eV^{-2}. The shape and uncertainty of such a partial cross section as a function of E is shown in Fig. 8. Stehman and Woo[17,18] introduced a zero core-contribution model which calculated not only the total but also the partial photodetachment cross section of polyatomic anions. They are currently doing a calculation of the photodetachment of NO_2^-. The partial cross section shown here can be compared to their results or similar calculations.

Our recommended values of E_A, r, and θ are insensitive to the following implicit factors in the data-analysis procedure. (1) Our results are insensitive to the number of terms used in the power series representation of the partial cross section. We checked the 3-, 4-, and 5-term representations. (2) Our results are insensitive to the assumed threshold behavior. The use of $(E - E_i)$ to the $\frac{1}{3}$ or $\frac{1}{4}$ power yields almost identical sets of (E_A, r, θ), but worse $\chi^2_{r,\,vis}$ and $\chi^2_{r,\,uv+vis}$ and much worse χ^2_{FC}.

An advantage of having a wide-range absolute

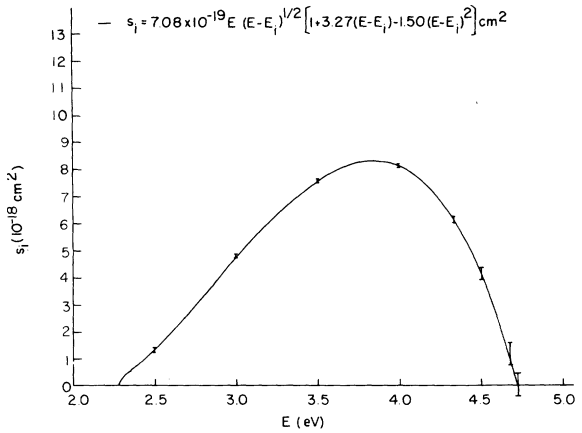

FIG. 8. Fitted partial photodetachment cross section of NO_2^- is shown. Uncertainties are indicated. Uncertainties beyond 4.4 eV depend strongly on the number of parameters used in the fitting and should therefore not be taken too rigorously.

magnitude photodetachment spectrum is that the structure constants obtained from a Franck-Condon factor analysis are likely to be unique. A proof of uniqueness is not offered here. However, we can show how a known nonuniqueness problem faced by another experimental technique[16] is resolved in the present work. A comparison of columns 2 and 5 of Table II shows that the values of calculated Franck-Condon factors are almost identical for two disparate sets of structure constants so far as the dominant progression, namely, the $(0, 0, 0 \rightarrow 0, \nu_2', 0)$ progression, is concerned. One set of structure constants has values of 1.15 Å and 119.5°. It is the set of constants identified here as being the structure constants of NO_2^- in the gas phase. The other set has a bond length which is 10 Å longer and a bond angle which is 3.5° smaller. The absolute magnitudes of corresponding Franck-Condon factors in the $(0, 0, 0 \rightarrow 0, \nu_2', 0)$ progression shown in these two columns differ by less than 2%. The differences in corresponding ratios of $F_{0,\nu_2',0}/F_{0,0,0}$ shown in these two columns are even smaller. The differences are less than 0.5%. Therefore, it is clear that the mere comparison of calculated ratios of $F_{0,\nu_2',0}/F_{0,0,0}$ against experimentally determined ratios of $F_{0,\nu_2',0}/F_{0,0,0}$ will not yield a unique set of structure constants, because the measured ratios of one particular progression are unlikely to have sufficient precision to perform such a demanding task. The Franck-Condon factors of such other progressions as the $(0, 0, 0 \rightarrow \nu_1', \nu_2', 0)$ progressions, where $\nu_1' \neq 0$ must be included, which is the case in this work. Table II shows that the corresponding values of Franck-

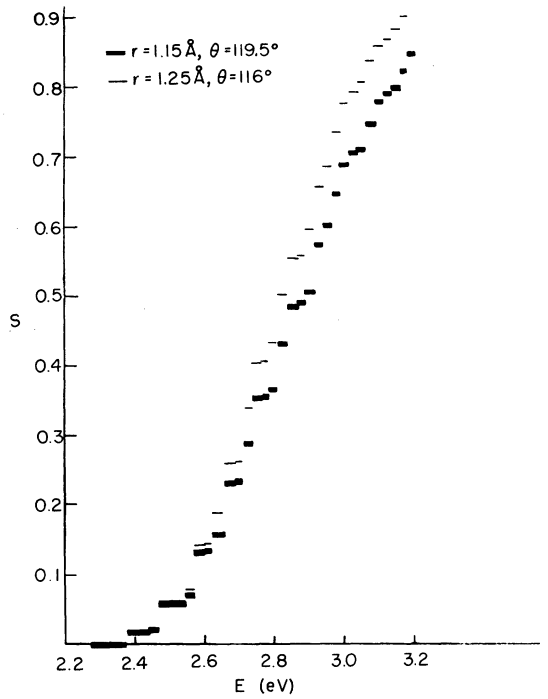

FIG. 9. Accumulated sum of Franck-Condon factors shown as a function of photon energy for two disparate sets of structure constants of NO_2^- at $E_A = 2.275$ eV.

Condon factors of these other progressions are significantly different for the two different sets of structure constants.

Figure 9 provides an illustration of why the energy range of the absolute photodetachment spectrum must be large, if one hopes to arrive at a unique set of structure constants using a Franck-Condon factor analysis. The accumulated sum of Franck-Condon factors S is calculated as a function of photon energy assuming that the only initial state is the (0, 0, 0) state of the ground electronic level of NO_2^-. The mathematical definition of S is shown in Eq. (11),

$$S(E, r, \theta) = \sum_{i=0}^{\infty} F_i(r, \theta) H(E - E_i) . \qquad (11)$$

Figure 9 shows a plot of S vs E for the two disparate sets of structure constants specified in the earlier paragraph. It shows that the values of S for the two sets are very similar over a photon energy range stretching from the electron affinity to about 2.6 eV, although Franck-Condon factors of all progressions have been included. However, at higher photon energies the rate of rise of the two sums becomes discernibly different. This difference causes the reduced χ^2's in our least-squares-fit programs to favor the (1.15 Å, 119.5°) set of structure constants so far as our measured photodetachment spectrum is concerned. Note that the rate of rise of a photodetachment cross-section spectrum depends implicitly on the rate of rise of S. A comparison of Eq. (10) and Eq. (11) will make apparent this dependence, thereby giving S a physical significance.

Structure constants of NO_2^- in the gas phase have not been measured previously. Comparison figures which are useful as background references are the structure constants of NO_2^- determined in crystalline structures of sodium nitrite[19] and those of the neutral NO_2 in the gas phase. They are shown in Table I. A few theoretical calculations of the structure constants of NO_2^- in the gas phase are available. An equation of motion calculation by Anderson and Simons[20] found $r = 1.26$ Å and $\theta = 118°$. An *ab initio* MOLCAO SCF calculation by Pfeiffer and Allen[21] found $\theta = 118°$ to 119° while keeping the O–N bond length at a constant value of 1.236 Å, which was the experimental value obtained for NO_2^- under interactive environment. O_3 is isoelectronic with NO_2^-. Its structure constants in the gas phase are $r = 1.2717$ Å and $\theta = 116.8°$.[22]

The electron affinity reported here is in good agreement with other recently reported values. Herbst *et al.*[5] reported a value of (2.36 ± 0.10) eV in their apparent cross-section study. In charge-transfer studies, Dunkin *et al.*[23] reported a value of (2.38 ± 0.06) eV whereas Hughes *et al.*[24] reported a value of (2.28 ± 0.10) eV.

VI. APPARENT PHOTODETACHMENT CROSS SECTION AS A FUNCTION OF TEMPERATURE

The apparent total cross section, which is the quantity measured in experiments having molecular ions in excited vibrational states, can be obtained from the expression,

$$\sigma_{app}(E) = \sum_j \rho_j \sum_i F_{ij} s_{ij}(E) \Big/ \sum_j \rho_j , \qquad (12)$$

where ρ_j is the density of NO_2^- in state j, and is the Boltzmann factor. Herbst *et al.*,[5] using $r = 1.236$ Å and $\theta = 115.4°$, deduced from their apparent cross-section data that the electron affinity of NO_2^- is 2.36 ± 0.10 eV. Using $E_A = 2.36$ eV, $T = 1500$ K, $(E - E_i)^{1/4}$ threshold behavior and calculated Franck-Condon factors based on $r = 1.236$ Å, $\theta = 115.4°$, their calculated apparent cross section fits the experimental data fairly well except at energies less than 2.4 eV. Figure 10 shows our calculated apparent cross section using $E_A = 2.275$ eV, $T = 2200$ K, $(E - E_i)^{1/2}$ threshold behavior and calculated Franck-Condon factors

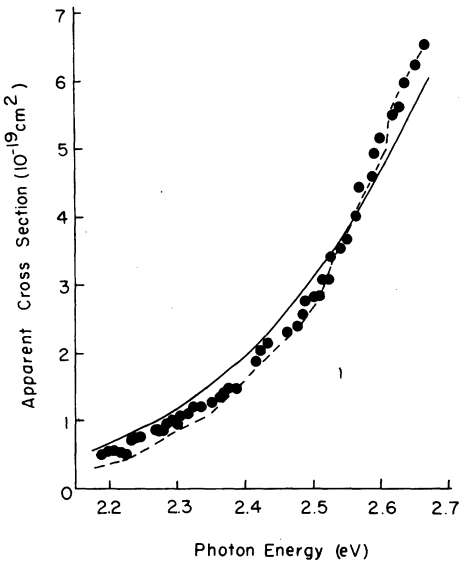

FIG. 10. The apparent photodetachment cross section measured by Herbst *et al.* is compared with two fitted curves based on substantially different values of E_A, r, θ, T, σ_0, and threshold behavior. The solid line represents the present work. The dotted line represents that of Herbst *et al.*

based on $r = 1.15$ Å and $\theta = 119.5°$. On the whole, our calculated apparent cross section shown in solid line seems to provide about the same quality fit to the experimental data as that of Herbst *et al.* shown in dashed lines. We interpret this to mean that our recommended values of E_A, r, and θ and the use of a one-half power threshold behavior are not contradictory to the apparent cross-section data seen in Fig. 10. If the assumption of a single vibrational temperature is valid, then our fit shows that the temperature of the NO_2^- beam used in the experiment of Herbst *et al.*[5] was as high as 2200 K. The theoretical interpretation of an apparent cross section may be a troublesome task. It tends to be ambiguous as a result of the lack of structure in the overall feature of the apparent cross section[25,26] and the uncertainties in the population distribution of initial states.

VII. SUMMARY

We have measured the absolute photodetachment cross section of NO_2^- in the visible and ultraviolet range. The molecular ions are in the ground electronic and vibrational state. The use of a pulsed dye laser in multipass configuration enabled observation of cross sections as small as 5×10^{-21} cm^2 in the visible and 1×10^{-18} cm^2 in the uv where laser output is very small. A two-dimensional harmonic Franck-Condon analysis gives the bond angle of NO_2^- to be $119.5°\pm1.0°$, the bond length to be 1.15 ± 0.02 Å, and the electron affinity to be 2.275 ± 0.025 eV. The partial cross section for each vibrational transition as a function of energy is roughly established.

No peroxy isomer of NO_2^- was observed. The solar photodetachment rate of NO_2^- is 0.042 ± 0.010 s^{-1} at 300 K based on the fitted total cross section shown in Fig. 7. Its value increases by 20% to 0.048 ± 0.012 s^{-1} at 2200 K based on our fitted curve shown in Fig. 10.

ACKNOWLEDGMENT

We thank William Clodius and Robert Stehman for helpful discussions; Dan Koon and N. K. Kang for writing the computer programs. This work was supported in part by National Science Foundation Grant No. ATM-T1-18324.

*Visitor; permanent address: Physics Department, Delaware State College, Dover, Delaware 19901.

[1]R. R. Corderman and W. C. Lineberger. Annu. Rev. Phys. Chem. 30, 347 (1979).
[2]P. Warneck, Chem. Phys. Lett. 3, 532 (1969).
[3]J. A. Vanderhoff, (unpublished).
[4]J. H. Richardson, L. M. Stephenson, and J. I. Brauman, Chem. Phys. Lett. 25, 318 (1974).
[5]E. Herbst, T. A. Patterson, and W. C. Lineberger. J. Chem. Phys. 61, 1300 (1974).
[6]G. P. Smith, L. C. Lee, and P. C. Cosby, J. Chem. Phys. 71, 4464 (1979).
[7]B. A. Huber, P. C. Cosby, J. R. Peterson, and J. T. Moseley, J. Chem. Phys. 66, 4520 (1976).
[8]S. F. Wong, T. V. Vorburger, and S. B. Woo, Phys. Rev. A 5, 2598 (1972).
[9]L. M. Branscomb, D. S. Burch, S. J. Smith, and S. Geltman, Phys. Rev. 111, 504 (1958).
[10]S. B. Woo, L. M. Branscomb, and E. C. Beaty, J. Geophys. Res. Space Physics 74, 2933 (1969).
[11]S. Geltman, Phys. Rev. 112, 176 (1958).
[12]E. P. Wigner, Phys. Rev. 73, 1002 (1948).
[13]K. J. Reed, A. H. Zimmerman, H. C. Anderson, and J. I. Brauman, J. Chem. Phys. 64, 1368 (1976).
[14]A. E. Douglas and K. P. Huber, Can. J. Phys. 43, 72 (1965).
[15]*CRC Handbook of Chemistry and Physics*, 58th ed. (C. R. C., Cleveland, 1977-78), p. E-63.
[16]S. E. Novick, P. C. Engelking, P. L. Jones, J. H. Futrell, and W. C. Lineberger, J. Chem. Phys. 70, 2652 (1979).
[17]R. M. Stehman and S. B. Woo, Phys. Rev. A 20, 281 (1979).
[18]R. M. Stehman and S. B. Woo, Phys. Rev. A 23, 2866 (1981).
[19]G. B. Carpenter, Acta Crystallogr. 8, 852 (1955).

[20]Earl Anderson and Jack Simons, J. Chem. Phys. 66, 2427–2430 (1977).
[21]G. V. Pfeiffer and L. C. Allen, J. Chem. Phys. 51, 190 (1969).
[22]K. M. Mack and J. S. Muenter, J. Chem. Phys. 66, 5268 (1977).
[23]D. B. Dunkin, F. C. Fehsenfeld, and E. E. Ferguson, Chem. Phys. Lett. 15, 257 (1972).
[24]B. M. Hughes, C. Lifshitz, and T. O. Tiernan, J. Chem. Phys. 59, 3162 (1973).
[25]S. Twomey, J. Franklin Inst. 279, 95 (1965).
[26]C. Russ, M. V. Barnhill III, and S. B. Woo, J. Chem. Phys. 62, 4420 (1975).